FAR-INFRARED EMISSION FROM DUST IN NORMAL GALAXIES

Richard J. Tuffs[1] **and Cristina C. Popescu**[2,3,4]

[1]Astrophysics Division, Max-Planck-Institut für Kernphysik, Saupfercheckweg 1, 69117 Heidelberg, Germany
[2]The Observatories of the Carnegie Institution of Washington, 813 Santa Barbara Str., Pasadena, 91101 California, USA
[3]IPAC(Caltech/JPL), 770 S. Wilson Avenue, Pasadena, California 91125, USA
[4]Research Associate, The Astronomical Institute of the Romanian Academy, Str. Cuţitul de Argint 5, Bucharest, Romania

ABSTRACT

We review the morphological and spectral energy distribution characteristics of the dust continuum emission (emitted in the 40 - 200 μm spectral range) from normal galaxies, as revealed by detailed ISOPHOT mapping observations of nearby spirals and by ISOPHOT observations of the integrated emissions from representative statistical samples in the local universe.

Key words: ISO

1. INTRODUCTION

The sensitivity of ISO and its spectral grasp extending to 200 μm made it the first observatory capable of routinely measuring the infrared emission corresponding to the bulk of starlight absorbed by interstellar dust in "normal"[1] galaxies. Here we review ISO's view of the morphological and spectral energy distribution (SED) characteristics of the dust continuum emission (emitted in the 40 - 200 μm spectral range) from normal galaxies, and its interpretation. In this review we only discuss the results from the ISOPHOT instrument (Lemke et al. 1996) on board ISO.

Although technically more demanding than observations in the Mid-Infrared (MIR) regime, only observations in the Far-Infrared (FIR) directly probe the role played by dust in the energy budget of star-forming galaxies. All star-forming galaxies are at least in part optically thick in the ultraviolet (UV)-optical regime, and the absorbed energy is predominantly re-radiated in the FIR. But the real investigative power of FIR astronomy lies in the fact that even for optically thin components of the interstellar medium, the large grains which dominate the FIR emission are in (or near to) equilibrium with the ambient interstellar radiation field (ISRF). Therefore, the grains act as test particles with FIR colours characteristic of the intensity and colour of the ISRF. This is illustrated in Fig. 1, which shows the predicted variation of infrared colours with radiation field intensities, for standard filter combinations of the ISOPHOT and ISOCAM instruments (on board ISO), and of the IRAS survey.

[1] We use the term "normal" to denote star-forming systems not undergoing a starburst, and not dominated by AGN activity.

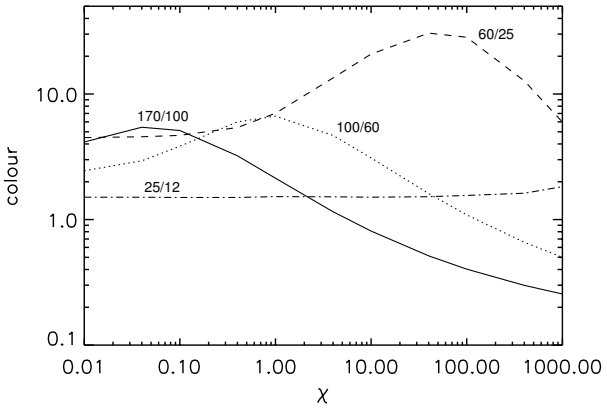

Figure 1. Predicted colour ratios for standard filter combinations 170/100 μm (solid line); 100/60 μm (dotted line); 60/25 μm (dashed line) and 25/12 μm (dot-dashed line) as a function of the strength of the local ISRF χ, where $\chi = 1$ near the sun. The calculations were made for spherical grains of astrophysical silicate, with the optical properties given by Laor & Draine (1993). A grain size distribution $n(a)\,da \propto a^{-3.5}$ was assumed, where a is the grain radius ($0.001 \leq a \leq 0.25$ μm). The colour of the radiation field illuminating the grains is fixed to that determined for the solar neighbourhood by Mezger, Mathis & Panagia (1982).

In particular, a filter set covering the range 60 to 170 μm probes intensities in the ISRF ranging from those expected for HII regions to those expected in the outskirts of disks of normal galaxies. By contrast, the MIR colour ratios are almost independent of the intensity of the ISRF, since they are determined by the relative abundance of small, impulsively heated grains.

2. ISOPHOT MAPPING OBSERVATIONS OF NEARBY SPIRALS

ISO represented a big improvement compared with IRAS in angular resolution, spectral grasp and sensitivity. Thus, in terms of imaging, the ISOPHOT instrument was able to make a better distinction between diffuse and discrete sources and their colours. Another point was the extension in wavelength coverage to 200 μm. In fact observations of nearby galaxies displayed a wide range of FIR colours between various morphological components, implying UV/optical/ near-infrared (NIR) interstellar radiation fields with a wide range of intensities and/-or colours:

Proceedings of the Symposium *"Exploiting the ISO Data Archive - Infrared Astronomy in the Internet Age"*, 24–27 June 2002, Sigüenza, Spain (C. Gry, S. B. Peschke, J. Matagne et al. eds., ESA SP-511)

– **Star formation regions**: HII regions ($40 \leq T_{\rm D} \leq 60$ K) and Parent Clouds ($15 \leq T_{\rm D} \leq 20$ K)
  – **Nuclear emission** ($T_{\rm D} \sim 30$ K)
  – **Diffuse Emission**: spiral arms and disk ($12 \leq T_{\rm D} \leq 20$ K)

These features appear to be general to nearby spirals mapped by ISOPHOT. They are perhaps best illustrated by the ISOPHOT map of M 31 (Haas et al. 1998), reproduced in Fig. 2. A ring of 10 kpc radius and a diffuse disk component are clearly seen on this image at 170 μm. The diffuse emission can be traced out to a radius of 22 kpc, so the galaxy has a similar overall size in the FIR as seen in the optical bands. In addition, there is a faint nuclear source, which is seen more prominently in HIRES IRAS 60 μm maps at similar resolution and in H_α. The overall SED, which is also constrained by a 240 μm COBE/DIRBE point, can be well described as a a superposition of two modified (m=2) Planck curves, with 16 and 45 K. The cold dust component at 16 K arises from both the ring structure (30%) and the diffuse disk (70%), illustrating the importance of the diffuse emission at least for this example. The 45 K component matches up well with HII region complexes in the ring structure. Associated with each HII region complex are also compact, cold emission sources (see Fig. 3 of Schmidtobreick, Haas & Lemke 2000) with dust temperatures in the 15 to 20 K range. These could well represent the parent molecular clouds in the star formation complexes which gave rise to the HII regions. Detailed examination of the morphology of the ring shows a smooth component of cold dust emission as well as the discrete cold dust sources.

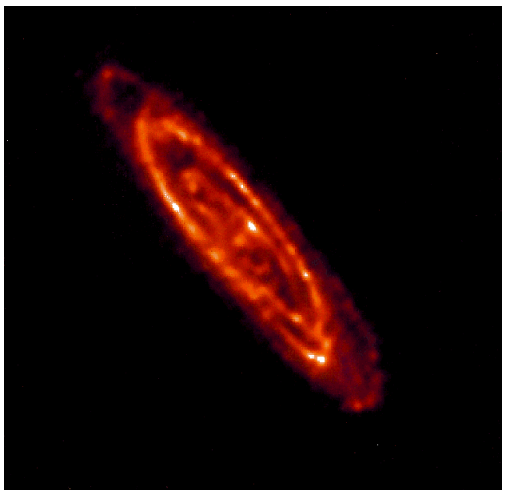

Figure 2. ISOPHOT 170 μm map of M 31 (Haas et al. 1998), with an angular resolution of 1.3 arcmin. North is towards the top, and East is towards the left. The field size is 2.9×2.9 *degrees.*

There are also beautiful datasets on normal galaxies which are more active in star formation than M 31, notably the Small Magellanic Cloud (type Sm), which was described by Bot et al. (2002) and by Wilke et al. (2002), and M 33 (type Scd; Hippelein et al. 2002). These galaxies also show a prominent diffuse cold dust component, upon which a warm dust component associated with HII region complexes is superimposed. The statistics of the HII region complexes are superior to those in M 31, and, in the case of M 33, the HII region complexes exhibit a trend for the 60:100 μm colour temperature to become colder with increasing galactocentric distance, as observed in our galaxy.

Preliminary results from ISOPHOT maps of nearby spiral galaxies were obtained by Tuffs et al. (1996) for NGC 6946, by Hippelein et al. (1996a,b) for M 51 and M 101 and for a sample of nearby galaxies by Alton et al. (1998b) and Davies et al. (1999). Claims by the latter two references that the FIR disks are more extended than the optical disks are not supported by the higher linear resolution maps of M 31 and M 33 nor by the deep map of NGC 891 (Popescu et al. 2001). However, the maps presented by Alton et al. (1998b) and Davies et al. (1999) were not corrected for transient effects of the detector, and therefore both the calibration and the derived scale lengths are uncertain.

In general there is a wealth of imaging data in the ISO archive still to be exploited, particularly from observations using the dedicated mapping "P32" astronomical observation template. Excellent photometric images are now becoming available for this mode, reduced using new software techniques (see for example the map of M 101 in Tuffs & Gabriel 2002a,b).

3. INTERPRETATION OF FIR EMISSION FROM NEARBY SPIRALS

The ISOPHOT imaging studies have directly demonstrated that spiral galaxies are inhomogeneous. Variations in FIR colours between the observed structures indicate ISRFs which vary by orders of magnitude in intensity. In general, this can be attributed to an inhomogeneous distribution of both emitters and absorbers. Large variations in the colour of the ambient UV-optical radiation field are also expected, especially if structures are optically thick to all or part of the stellar light. Since the absorption probability of stellar photons by grains is a strong function of wavelength, this will also give rise to strong variations in the intensity and colour of the FIR emission. A quantitative interpretation of the FIR emission therefore requires realistic models for the propagation of stellar photons in galaxian disks, to calculate both the colour and intensity of radiation fields illuminating grains.

George Helou described the semi-empirical model of Dale & Helou (2002), which assumes a power law distribution of dust masses over UV-optical radiation energy densities (all of a common intrinsic colour). This model can reproduce observed trends in the MIR-FIR-submm colours of statistical samples, and has also been used to extract bolometric IR emission and dust masses from the ISO data. However, a quantitative interpretation of dust emission in terms of star formation rates and star formation histories requires a combined analysis of the UV-optical/FIR-submm SEDs, embracing a self-consistent model for the propagation of the photons.

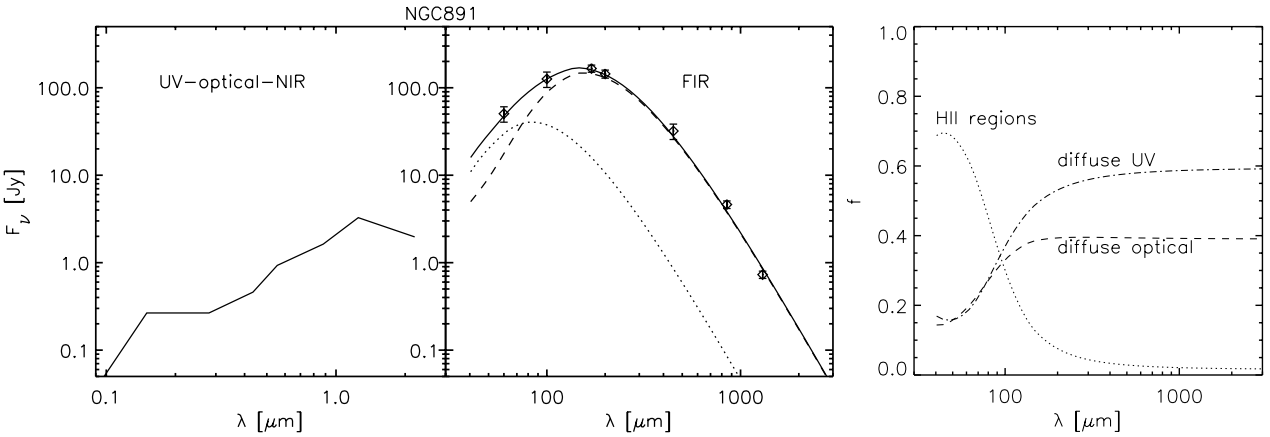

Figure 3. a) The predicted SED of NGC 891 from Popescu & Tuffs (2002a), for a model with $SFR = 3.8\,\mathrm{M}_\odot$*/yr,* $F = 0.22$ *and* $M_{\rm dust} = 7 \times 10^7\,\mathrm{M}_\odot$ *LH panel: the intrinsic emitted stellar radiation (as would have been observed in the absence of dust). RH panel: the re-radiated dust emission, with diffuse and HII components plotted as dashed and dotted lines, respectively. The data (integrated over* $\pm 225'$ *in longitude), are from Alton et. al 1998a (at 60, 100, 450 & 850* μ*m), Guélin et al. 1993 (at* 1300 μ*m) and from Popescu & Tuffs (2002a) (at 170 & 200* μ*m). b) The fractional contribution of the three stellar components to the FIR emission, calculated for the case of NGC 891.*

There are several such models in use which incorporate various geometries for the stellar populations and dust. We will concentrate here on the model of Popescu et al. (2000a), since this is the only model where the geometry of the dust and stellar populations is directly constrained by the optical images. It is furthermore the only model which has been used to make direct predictions for the spatial distribution of the FIR emission for comparison with the ISO images. Full details of the model are given by Popescu et al. (2000a), Misiriotis et al. (2001) and Popescu & Tuffs (2002a). In brief, the model includes solving the radiative-transfer problem for a realistic distribution of absorbers and emitters, considering realistic models for dust, taking into account the grain-size distribution and stochastic heating of small grains and the contribution of HII regions. The FIR-submm SED is fully determined by just three parameters: the star-formation rate SFR, the dust mass $M_{\rm dust}$ associated with the young stellar population, and a factor F, defined as the fraction of non-ionising UV photons which are locally absorbed in HII regions around the massive stars.

Here we illustrate this model with the example of the edge-on galaxy NGC 891. The model can however be applied to galaxies of any inclination. The best fit obtained for the FIR-submm SED of NGC 891 is shown in the right hand panel of Fig. 3a.

If L_0 is the intrinsic UV luminosity corresponding to unity SFR, the relation between the FIR luminosity $L_{\rm FIR}^{\rm tot}$ and SFR can be described by:

$$L_{\rm FIR}^{\rm tot} = L_{\rm FIR}^{\rm HII} + L_{\rm FIR}^{\rm UV} + L_{\rm FIR}^{\rm opt}$$

$$L_{\rm FIR}^{\rm tot} = SFR \times L_0 \times F + SFR \times L_0 \times (1-F) \times G_{uv} + \\ + L_{\rm FIR}^{\rm opt}$$

where G_{uv}, which also depends on $M_{\rm dust}$, is the probability that a non-ionising UV photon released into the diffuse dust will be absorbed there.

It can be seen that a natural outcome of this modelling technique is the prediction of a diffuse cold component of dust emission powered by a combination of non-ionising UV and optical-NIR photons, and a warm component of dust emission corresponding to the ensemble of discrete HII regions. This corresponds to what we have seen in the ISOPHOT maps of nearby galaxies.

The model also predicts the relative contributions of the young and old stellar populations to the dust emission as a function of FIR wavelength (Fig. 3b). An increase in the relative importance of UV heating in the diffuse dust emission component towards longer wavelengths is apparent. This arises because the coldest grains are those which are in weaker radiation fields, either in the outer optically thin regions of the disk or because they are shielded from radiation by optical depth effects. In the first situation the absorption probabilities of photons are controlled by the optical properties of the grains, so the UV photons will dominate the heating. The second situation arises for dust associated with the young stellar population, where the UV emissivity far exceeds the optical emissivity.

This analysis, together with the observational evidence from the maps produced by ISOPHOT, throws new light on the physical interpretation of the 60:100 μm ratio, which is commonly used as a gauge of star formation activity (Helou & Lonsdale 1987). This ratio has to be understood in terms of the inhomogeneous nature of disks in the FIR. Thus, the emission at 60 μm mainly traces locally heated warm grains in and around HII regions, whereas the emission at 100 μm mainly traces the

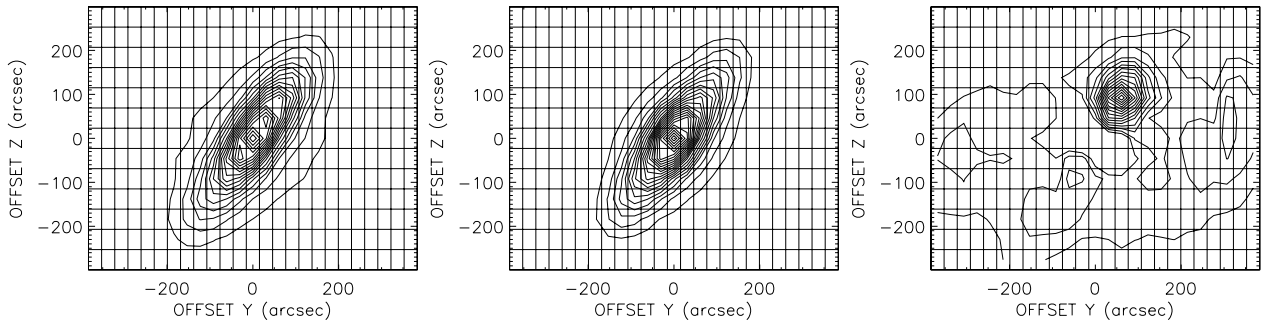

Figure 4. a) Contour plot of the observed brightness distribution of NGC 891 at 170 μm (Popescu & Tuffs 2002a). The contours are plotted from 10.7 to 230.0 MJy/sr in steps of 12.2 MJy/sr. The grid indicates the actual measured sky positions sampled at $31 \times 46'$ in the spacecraft coordinates Y and Z. b) Contour plot of the simulated diffuse brightness distribution of NGC 891 at 170 μm. The contours are plotted from 10.4 to 239.7 MJy/sr in steps of 10.4 MJy/sr. c) Contour plot of the observed minus simulated diffuse brightness distribution of NGC 891 at 170 μm. The contours are plotted from 2.2 to 46.1 MJy/sr in steps of 3.1 MJy/sr. The unresolved source from the Northern side of the galaxy and the faint extended source from the Southern side account for 8% of the integrated flux density, in agreement with the model prediction for FIR localised sources at this wavelength.

emission from the diffuse dust, powered by optical photons as well as by (non-ionising) UV photons.

A particularly stringent test of the model is to compare its predictions for the morphology of the diffuse dust emission component near the peak in the FIR SED with spatially resolved maps. This comparison is shown in Fig. 4a,b, again for the case of NGC 891. A remarkable agreement between the maps is apparent. The residual map between the observed and the simulated maps of the diffuse component (Fig. 4c) reveals a compact source on the Northern side of the galaxy (and a faint extended source seen in the Southern side), with integrated fluxes in agreement with the model predictions for localised sources. The excess emission in the northern side may be a giant molecular cloud complex associated with one of the spiral arms. The remaining diffuse emission is at a level of 1% of the peak brightness and is probably attributable to residual detector artifacts.

4. ISOPHOT OBSERVATIONS OF STATISTICAL SAMPLES

A total of 31 hours of the ISO mission was dedicated to ISOPHOT pointed observations of statistical samples of local universe galaxies. All these projects were complementary in terms of selection and observational goals. In descending order of depth, the published surveys are: the ISOPHOT Virgo Cluster Deep Survey (63 galaxies), the Coma/A1367 Survey (18 galaxies) and the ISO Bright Spiral Galaxies Survey (77 galaxies). In addition, 115 galaxies have been catalogued from the Serendipity Survey. Furthermore, the statistical sample of 60 bright galaxies studied spectroscopically by LWS by Malhotra et al. (2001) was also observed by ISOPHOT at 170 μm with short stares, but the photometry is not yet published.

The ISOPHOT Virgo Cluster Deep Survey (Tuffs et al. 2002; Popescu et al. 2002) represents the *deepest survey* (both in luminosity and surface brightness terms) of normal galaxies yet measured in the FIR. A complete volume- and luminosity sample of 63 gas-rich Virgo Cluster galaxies selected from the Virgo Cluster Catalog (Binggeli, Sandage & Tammann 1985; see also Binggeli, Popescu & Tammann 1993) with Hubble types later than S0 and brighter than $B_{\rm T} \leq 16.8$ were measured with ISOPHOT at 60, 100 and 170 μm. Deep oversampled P32 strip maps covered the entire optical extent of each target (down to the 25.5 mag arcsec^{-2} B-band isophote) as well as adjacent background directions. The faintest detected emissions from the survey are 50, 40 and 80 mJy at 60, 100 and 170 μm, respectively. The total on target time (ISOPHOT) for the survey was 20 hours. The sample was also mapped by ISOCAM (Boselli et al. 1997) and was (in part) observed by LWS (Leech et al. 1999).

The ISOPHOT Virgo Cluster Deep Survey is providing the basis for statistical investigations of the FIR spectral energy distributions of gas rich galaxies in the local universe spanning a broad range in star-formation activity and morphological types, including dwarf systems and galaxies with rather quiescent star formation activity.

The Coma/A1367 Survey (Contursi et al. 2001) consists of 6 spiral and 12 irregular galaxies having IRAS detections at 60 μm. The galaxies were selected to be located within 2 or 1 degrees of the X-ray centres of Coma and A1367 clusters, respectively, with emphasis on peculiar optical morphologies. Each galaxy was observed in a single pointing, by chopping between the galaxy and a background direction. The data were taken at 60, 80, 100, 120, 170 and 200 μm (but only reduced for 120, 170 and 200 μm) for a total on target time (ISOPHOT) of 2 hr. The sample, also observed with ISOCAM, provided a

database of integrated flux densities for a pure cluster sample of high luminosity spiral and irregular galaxies.

The ISO Bright Spiral Galaxies Survey (Bendo et al. 2002a) consists of 77 spiral and S0 galaxies chosen from the Revised Shapley-Ames Catalog (RSA), with $B_{\rm T} \leq 12.0$. Almost all are IRAS sources. Mainly an ISOCAM survey, the project also used 7 hr of on target ISOPHOT time to take 60, 100 and 170 μm short stares towards the nucleus of the galaxies and towards background fields. The sample provides a database of FIR surface brightnesses of the central regions of bright spiral galaxies, including S0s.

The ISO Bright Spiral Galaxies Survey and the ISOPHOT Virgo Cluster Deep Survey represent the principle investigations of optical selected samples of normal galaxies. It should be emphasised that the main difference between them is primarily one of shallow versus deep, rather than field versus cluster, since by design the Virgo Sample predominantly consists of infalling galaxies from the field, and no cluster specific effects could be found.

The Serendipity Survey (Stickel et al. 2000) has so far catalogued 115 galaxies with $S_\nu \geq 2$ Jy at 170 μm and with morphological types predominantly S0/a - Scd. This sample provides a database of integrated 170 μm flux densities for relatively high luminosity spiral galaxies, all detected by IRAS at 60 & 100 μm. A more detailed description of this survey was given in the presentation of Stickel (Stickel et al. 2002a).

5. INTERPRETATION OF FIR EMISSION FROM STATISTICAL SAMPLES

The emerging result of all ISOPHOT statistical studies was that the SEDs of normal galaxies in the 40 - 200 μm spectral range require both warm and cold dust emission components to be fitted. First indications of this result were given by the multi-filter ISOPHOT photometry obtained for 8 inactive spiral galaxies (Krügel et al. 1998; Siebenmorgen, Krügel & Chini 1999). Stickel et al. (2000) and Contursi et al. (2001) found a cold dust component for most of the galaxies in their samples (The Serendipity and the Coma/A1367 samples, respectively), for which upper limits for the cold dust temperatures were inferred. The cold dust component is most prominent in the most "quiescent" galaxies, like those contained in the ISOPHOT Virgo Cluster Deep sample, where the cold dust temperatures were found to be broadly distributed, with a median of 18 K (Popescu et al. 2002), some 8 - 10 K lower than would have been predicted by IRAS. The corresponding dust masses were correspondingly found to be increased by factors of typically 2 - 10 (Stickel et al. 2000) for the Serendipity Sample and by factors 6 - 13 (Popescu et al. 2002) for the Virgo Sample, with respect with previous IRAS determinations. As a consequence, the derived gas-to-dust ratios are much closer to the canonical value of $\sim$ 160 for the Milky Way (Stickel et al. 2000, Contursi et al. 2001), but with a broad distribution of values (Popescu et al. 2002). The FIR properties of the analysed galaxies do not seem to be affected by the environment (Contursi et al. 2001).

Of particular interest are the results concerning the trends with Hubble type found by Popescu et al. (2002) for the ISOPHOT Virgo Cluster Deep sample. A tendency was found for the temperatures of the cold dust component to become colder, and for the cold dust surface densities (normalised to optical area) to increase with increasing lateness in the Hubble type (Figs. 5a,b). A particularly surprising result was the low dust temperatures (ranging down to less than 10 K) and large dust masses associated with the Virgo Im and Blue Compact Dwarf (BCD) galaxies. Another important trend is the increase of the normalised (to K$'$ band magnitude) FIR luminosity as we progress from the early to the later Hubble types (Fig. 5c). This result was later confirmed by Bendo et al. (2002b) for the RSA sample. A related result was also obtained by Pierini et al. (1999) for the LWS data on Virgo galaxies, where a strong correlation of normalised [CII] emission with Hα equivalent widths was interpreted as a trend of increasing star-formation rate along the Hubble sequence.

Finally, Popescu & Tuffs (2002b) also found an increase of the ratio of the dust emission to the total stellar emitted output along the Hubble sequence. This correlation is quite strong, ranging from typical values of $\sim 15\%$ for early spirals to up to $\sim 50\%$ for some late spirals (Popescu & Tuffs 2002b). This, together with the trend for a decrease in the temperature of the cold dust, would suggest a trend of increasing opacities with increasing star-formation activity. The extreme BCDs can have even higher percentages of their bolometric output re-radiated in the thermal infrared. This correlation can be also interpreted as a sequence from normal to dwarf gas rich galaxies, with the dwarfs having an increased contribution of the FIR output to the total bolometric output. These findings could be important for our perception of the distant Universe, where, according to the hierarchical galaxy formation scenarios, gas rich dwarf galaxies should prevail. We would then expect these galaxies to make a higher contribution to the total FIR output in the early Universe than previously expected.

6. DUST OUTSIDE GALAXIES

In some systems dominated by cold dust emission there is evidence that the cold dust emission is external to any optically emitting region and/or that dust is supplied from an external dust reservoir.

Thus, the unexpected result that large amounts of cold dust exist in some Virgo BCDs (Popescu et al. 2002) was interpreted as being indicative of dust surrounding the optical galaxy, originating in an external dust reservoir. In fact, in two cases direct evidence was found of resolved emission at 170 micron on scales of up to 10 kpc. The BCD galaxies were found to have the highest dust mass surface densities (normalised to optical area) and the coldest dust temperatures of the galaxies in the sample. This is a particularly unexpected result, since the IRAS observations of BCDs could be accounted for in terms of dust heated locally in HII regions, with temperatures of 30 K or more. To qualitatively account for the FIR and optical extinction characteristics of BCDs, Popescu et al. (2002) pro-

Figure 5. Trends with Hubble type for the ISOPHOT Virgo Cluster Deep sample (Popescu et al. 2002). The distribution of a) cold dust temperatures $T_{\rm D}^{\rm cold}$; b) cold dust mass surface densities $M_{\rm D}^{\rm cold}/D^2$; c) normalised FIR luminosity (to the K' band magnitude) for different Hubble types. The hatched histograms represent the distributions for the galaxies with SEDs fitted by only one dust component. The filled histograms represent the distributions for the galaxies with detections only at 100 and 170 μm.

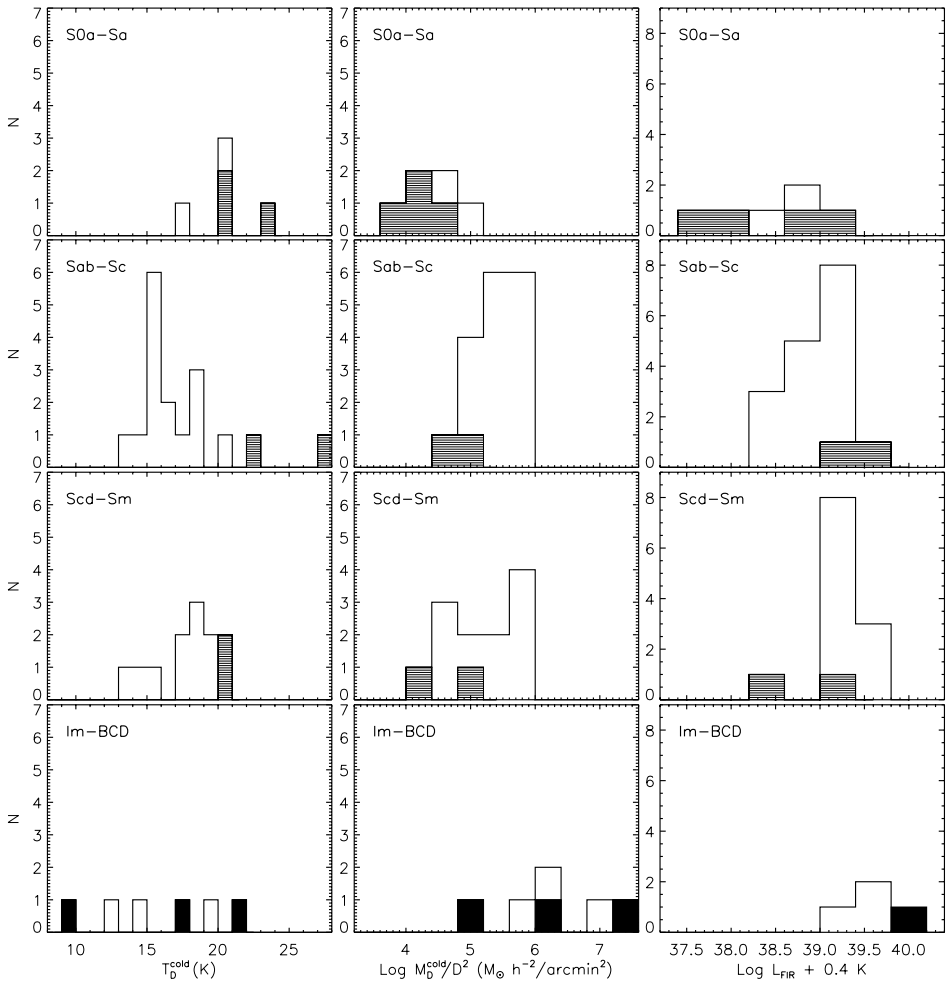

(a) (b) (c)

posed two scenarios invoking collisionally or photon-heated emission from grains originating in the surrounding intergalactic medium. In the one scenario, grains are swept up from a surrounding protogalactic cloud and heated collisionally in an optically thin wind bubble blown from the BCD. In the other, the grains are taken to be photon-heated in an optically thick disk surrounding the optical galaxy. The disk is indicative of a massive gas/dust accreting phase which makes dwarf galaxies sporadically bright optical-UV sources when viewed out of the equatorial plane of the disk. In both scenarios the dust does not have a galactic origin, but needs to exist in the immediate vicinity of the galaxies, where it can either be heated by winds or can accrete into the dwarfs.

Dust outside galaxies has also been discovered in a deep ISOPHOT survey of a field centred on the giant elliptical galaxy M86 in the Virgo cluster by Stickel et al. (2002b). One of the sources of FIR emission seen in the periphery of the field is extremely cold and has no obvious optical counterpart. It could trace a dust-rich "relic" of the interstellar media of two spiral galaxies removed in an interaction as postulated by Völk & Xu (1994). Such objects could themselves undergo localised

episodes of star formation and could conceivably account for the large dust masses associated with the Virgo BCDs.

Moving more in the direction of the intragroup medium, the classical example is Stephan's Quintet (SQ), mapped by ISOPHOT using its oversampling mapping mode P32. The 60 μm map (Sulentic et al. 2001) and the 100 μm map (Xu & Tuffs 2002) show the probable detection of FIR diffuse emission from the intragroup medium. In particular the 100 μm map shows clear evidence for extended FIR emission in the periphery of SQ, its morphology having a striking resemblance to the morphology of the diffuse synchrotron radio emission. Since the diffuse radio emission very probably traces a large scale shock in the intragroup medium, the diffuse FIR emission is likely to be also associated with the passage of the shock front. Such an association was predicted by Popescu et al. (2000b) for the case of large-scale accretion shocks in clusters.

ACKNOWLEDGEMENTS

We thank Dr. Jörg Fischera for providing us with Fig. 1, and Prof. Heinrich Völk, for informative discussions.

REFERENCES

Alton P.B., Bianchi S., Rand R.J., et al., 1998a, ApJ, 507, L125
Alton, P.B., Trewhella, M., Davies, J.I., et al. 1998b, A&A, 335, 807
Bendo, G.J., Joseph, R.D., Wells, M. et al. 2002a, AJ 123, 3067
Bendo, G.J., Joseph, R.D., Wells, M. et al. 2002b, AJ in press
Binggeli, B., Popescu, C.C. & Tammann, G.A. 1993, A&AS, 98, 275
Binggeli, B., Sandage, A. & Tammann, G.A. 1985, AJ, 90, 1681
Bruzual, G. & Charlot, S. 1993, ApJ, 405, 538
Boselli, A., Lequeux, J., Contursi, A. et al. 1997, A&A, 324, L13
Bot, C. et al. 2002, this volume
Contursi, A., Boselli, A., Gavazzi, G. et al. 2001, A&A 365, 11
Dale, D. & Helou, G. 2002, ApJ in press
Davies, J.I., Alton, P., Trewhella, M., Evans, R., & Bianchi, S. 1999, MNRAS, 304, 495
Guélin, M., Zylka, R., Mezger, P.G., et al., 1993, A&A, 279, L37
Haas, M., Lemke, D., Stickel, M., et al. 1998, A&A, 338, L33
Helou, G. 2002, this volume
Helou, G. & Lonsdale, C. 1987, ApJ 314. 513
Hippelein, H., Lemke, D., Tuffs, R.J., et al. 1996a, A&A, 315, L79
Hippelein, H., Lemke, D., Haas, M., et al. A&A, 315, L82
Hippelein, H. et al. 2002, in preparation
Kylafis, N.D., & Bahcall, J.N. 1987, ApJ, 317, 637
Krügel, E., Siebenmorgen, R., Zota, V., & Chini, R. 1998, A&A, 331, L9
Laor A., & Draine B. T. 1993, ApJ 402, 441
Leech, K.J., Völk, H.J., Heinrichsen, I., et al. 1999, MNRAS, 310, 317
Lemke, D., Klaas, U., Abolins, J. et al. 1996, A&A, 315, L64
Malhotra, S., Kaufman, M.J., Hollenbach, D., et al. 2001, ApJ 561, 766
Mezger P.G., Mathis J.S., Panagia N., 1982, A&A 105, 372
Misiriotis A., Popescu, C.C., Tuffs, R.J., & Kylafis, N.D. 2001, A&A, 372, 775
Pierini, D., Leech, K.J., Tuffs, R.J., & Völk, H.J. 1999, MNRAS 303, L29
Popescu, C.C., Misiriotis A., Kylafis, N.D., Tuffs, R.J., & Fischera, J., 2000a, A&A, 362, 138
Popescu, C.C., Tuffs, R.J., Fischera, J. & Völk, H.J. 2000b, A&A, 354, 480
Popescu, C.C., Madore, B.F., Tuffs, R.J., & Kylafis, N.D. 2001, AAS198, 76.01
Popescu, C.C. & Tuffs, R.J. 2002a, Reviews in Modern Astronomy, vol 15.
Popescu, C.C. & Tuffs, R.J. 2002b, MNRAS Letters, in press
Popescu, C.C., Tuffs, R.J., Völk, H.J., Pierini, D. & Madore, B.F., 2002, ApJ 567, 221
Schmidtobreick, L., Haas, M., & Lemke, D. 2000, A&A 363, 917
Siebenmorgen, R., Krügel, E., & Chini, R. 1999, A&A, 351, 495
Stickel, M., Lemke, D., Klaas, U. et al. 2000, A&A 359, 865
Stickel, M. et al. 2002a, this volume
Stickel, M. et al. 2002b, in preparation
Sulentic, J.W., Rosaldo, M., Dultzin-Hacyan, D., et al. AJ 122, 2993, 2001
Tuffs, R.J. & Gabriel, C., 2002a, in Proc. "ISOPHOT Workshop on P32 Oversampled Mapping", ESA SP-482
Tuffs, R.J. & Gabriel, C., 2002b, this volume
Tuffs, R.J., Popescu, C.C., Pierini, D., et al. 2002, ApJS 139, 37
Tuffs, R.J., Lemke, D., Xu, C., et al. 1996, A&A, 315, L149
Völk, H.J. & Xu, C. 1994 Infrared Phys. Technol., 35, 527
Wilke, K. et al. 2002, this volume
Xu, C. & Tuffs, R.J. 2002, in: "Proc. ISOPHOT Workshop on P32 Oversampled Mapping", ESA SP-482